

Design, synthesis and biological evaluation of novel thiazole-naphthalene derivatives as potential anticancer agents and tubulin polymerisation inhibitors

Guangcheng Wang^a , Wenjing Liu^{a,b}, Meiyang Fan^{a,b}, Min He^{a,b}, Yongjun Li^c and Zhiyun Peng^d

^aState Key Laboratory of Functions and Applications of Medicinal Plants, Guizhou Provincial Key Laboratory of Pharmaceutics, Guizhou Medical University, Guiyang, China; ^bSchool of Pharmacy, Guizhou Medical University, Guiyang, China; ^cEngineering Research Center for the Development and Application of Ethnic Medicine and TCM (Ministry of Education), Guizhou Medical University, Guiyang, China; ^dCollege of Food Science and Technology, Shanghai Ocean University, Shanghai, China

ABSTRACT

A novel series of thiazole-naphthalene derivatives as tubulin polymerisation inhibitors were designed, synthesised, and evaluated for the anti-proliferative activities. The majority of the tested compounds exhibited moderate to potent antiproliferative activity on the MCF-7 and A549 cancer cell lines. Among them, compound **5b** was found to be the most active compound with IC₅₀ values of 0.48 ± 0.03 and 0.97 ± 0.13 μM. Moreover, mechanistic studies revealed that **5b** significantly inhibited tubulin polymerisation with an IC₅₀ value of 3.3 μM, as compared to the standard drug colchicine (IC₅₀ = 9.1 μM). Further cellular mechanism studies elucidated that **5b** arrested the cell cycle at G2/M phase and induced apoptosis in MCF-7 cancer cells. Molecular modelling study indicated that **5b** binds well to the colchicine binding site of tubulin. In summary, these results suggest that **5b** represents a promising tubulin polymerisation inhibitor worthy of further investigation as potential anticancer agents.

ARTICLE HISTORY

Received 3 April 2021
Accepted 16 July 2021

KEYWORDS

Thiazole; naphthalene; tubulin; anticancer; tubulin polymerisation

1. Introduction





Microtubules are a component of the cytoskeleton, which is formed through the polymerisation of α - and β -tubulin heterodimers¹. They play an important role in a wide range of cellular processes such as cell proliferation, cellular transport, intracellular trafficking, and angiogenesis^{2–4}. In the cellular microtubule system, microtubule formation is a dynamic equilibrium related to the polymerisation and depolymerisation of α , β -tubulin heterodimers⁵. Disrupting the tubulin dynamics equilibrium blocks the cell division at mitosis and thus resulting in the cell cycle arrest at metaphase, which leads to cell death^{6,7}. Moreover, cancer cells are more in the division phase than normal cells, which means that they are more prone to anti-tubulin agents⁸. Therefore, microtubules have become an attractive target for the design and development of novel anticancer agents^{9–11}.


Thiazole is an important heterocyclic scaffold widely found in a range of synthetic bioactive molecules, which has attracted considerable attention in drug discovery over the past decade. Thiazole derivatives displayed a wide range of pharmacological activities, such as anticancer, anti-inflammatory, antioxidant, antimicrobial, anti-HIV, and antibacterial activities^{12–14}. Several thiazole-containing drugs have been approved for clinical use, such as sulphathiazole, ravuconazole, ritonavir, and meloxicam. It's important to note that thiazole could be used as a promising scaffold for the development of anticancer agents^{15–17}. Over the last few years, numerous thiazole derivatives have been reported to show

potent anticancer activity by inhibiting tubulin polymerisation (Figure 1, I–IV)^{18–21}.

On the other hand, naphthalene is a prominent core structure in many anticancer agents. A number of naphthalene derivatives have been reported as potent inhibitors of tubulin (Figure 1, V–VIII)^{22–25}. Such as Maya et al. reported the synthesis of a series of new naphthalene analogues of combretastatin A-4 (CA-4) and the most cytotoxic naphthalene analogues **V** exerted tubulin polymerisation inhibition activity and arrest cell cycle in G2/M phase in human cancer cells²⁵. Based on the lead compound HMNC-74, we synthesised a series of new naphthalene-chalcone derivatives and evaluated their anticancer activity. Among them, compound **IV** was the most potent tubulin polymerisation inhibitor with an IC₅₀ value of 8.4 μM²³. Recently, we have also reported a new series of benzophenone derivatives bearing naphthalene moiety, and compound **VII** displayed potent antiproliferative activity against various cancer cell lines by targeting tubulin colchicine binding site²⁴. Furthermore, we also designed a new series of chalcones containing naphthalene moiety (**VIII**) based on natural tubulin inhibitor millepachine^{22,26}.

Molecular hybridisation approach is an efficient and often used method for the design and development of new therapeutic agents in the current medicinal chemistry research^{27–30}. Encouraged by these observations and in continuation of our interest in the discovery of tubulin inhibitors, herein we reported the synthesis of a novel series of thiazole-naphthalene derivatives by hybridisation of thiazole moiety with naphthalene structural

CONTACT Guangcheng Wang  wanggch123@163.com  State Key Laboratory of Functions and Applications of Medicinal Plants, Guizhou Provincial Key Laboratory of Pharmaceutics, Guizhou Medical University, Guiyang, China; Zhiyun Peng  pengzhiyun1986@163.com  College of Food Science and Technology, Shanghai Ocean University, Shanghai, China

 Supplemental data for this article can be accessed [here](#).

© 2021 The Author(s). Published by Informa UK Limited, trading as Taylor & Francis Group.

This is an Open Access article distributed under the terms of the Creative Commons Attribution License (<http://creativecommons.org/licenses/by/4.0/>), which permits unrestricted use, distribution, and reproduction in any medium, provided the original work is properly cited.

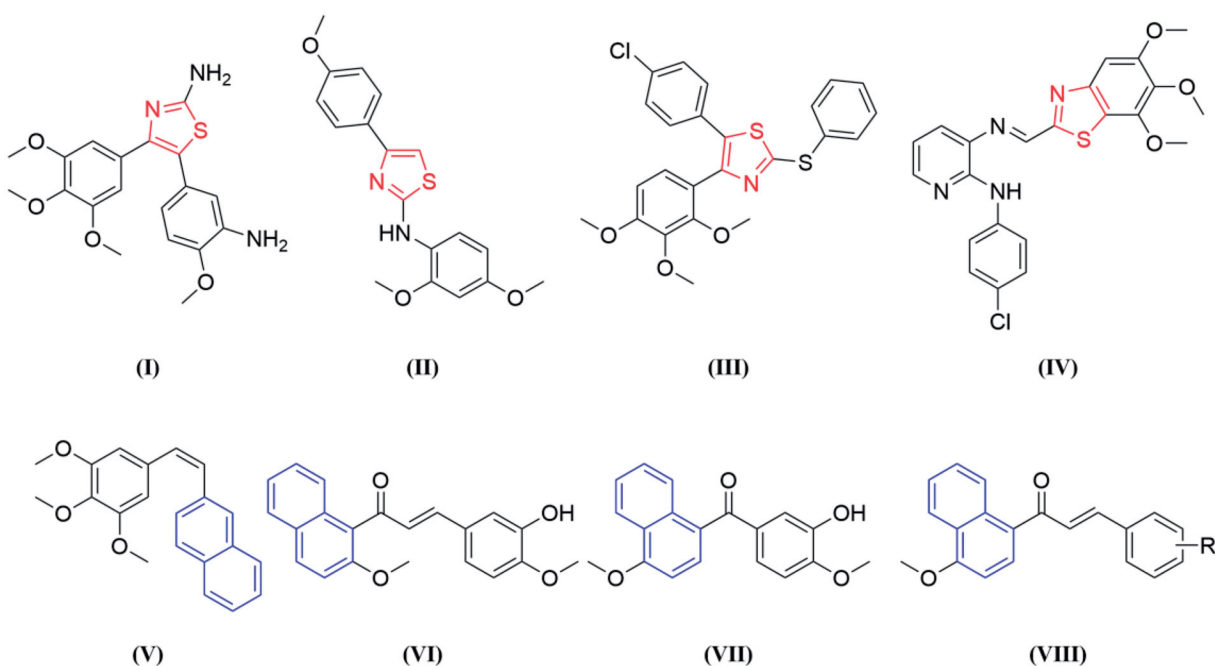


Figure 1. Some tubulin polymerisation inhibitors containing thiazole or naphthalene moiety.

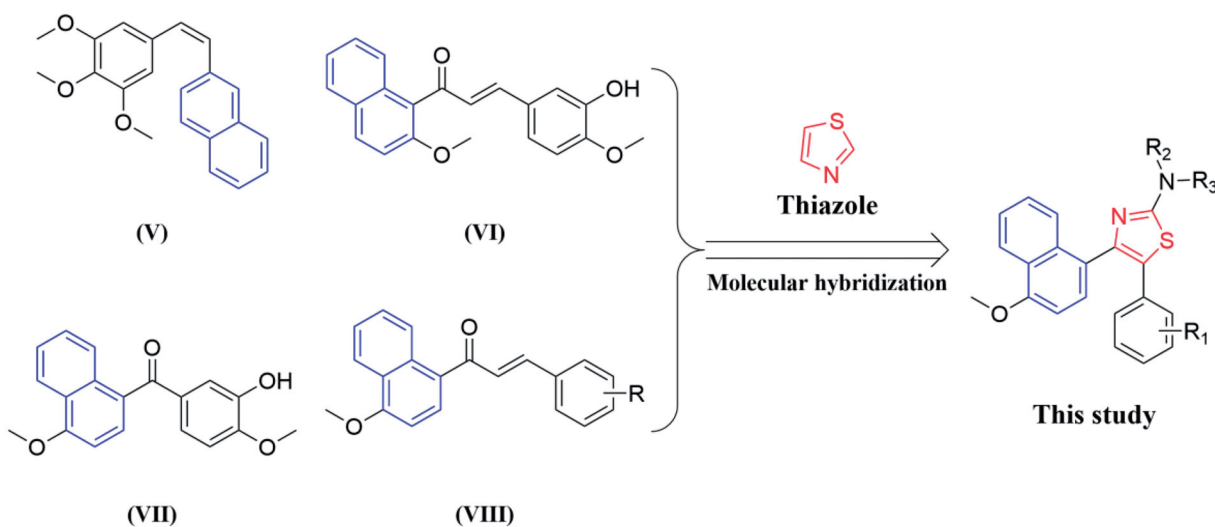


Figure 2. The design strategy of the target compounds in this study.

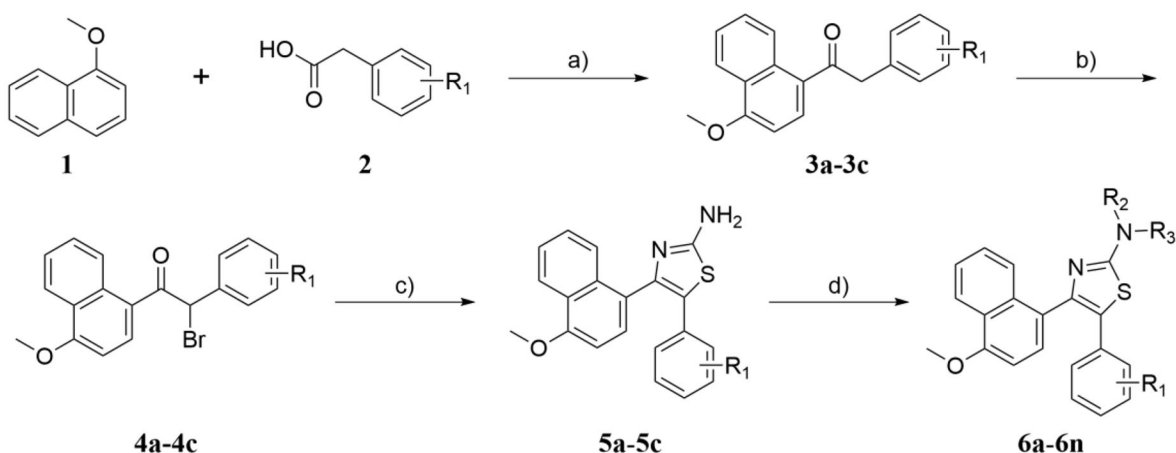
motif into a single molecule and examined their antiproliferative and antitubulin effects (Figure 2).

2. Chemistry

A series of thiazole-naphthalene derivatives (**5a–5c** and **6a–6n**) were synthesised according to the pathways described in Scheme 1. Deoxybenzoins **3a–3c** was prepared by condensation of 1-methoxynaphthalene **1** with appropriate phenylacetic acids **2** in the presence of trifluoroacetic anhydride (TFAA) in trifluoroacetic acid (TFA) at room temperature. Treatment of **3a–3c** with pyridinium tribromide in CH_2Cl_2 to give compounds **4a–4c**. Then, condensation of **4a–4c** with thiourea under reflux in ethanol to afford the title compounds (**5a–5c**) in high yields. Finally, a series of thiazole-naphthalene derivatives (**6a–6n**) were prepared by a condensation reaction of **5a–5c** with a variety of commercially available

acid anhydride. All of the title compounds are new and not reported in the literature to date.

The structures of all the title compounds (**5a–5c** and **6a–6n**) were characterised by ^1H NMR, ^{13}C NMR, and HRMS (Supplementary material). For instance, the ^1H NMR spectrum of compound **5a** shown two singlets at δ 3.68 and δ 3.99 due to two methoxy groups in the aromatic ring. The single peak of NH_2 group was observed at δ 5.59 ppm. Two doublet peaks at δ 6.59 and δ 6.94 with coupling constant of 8.8 Hz were attributed to the aromatic protons of C3,5-H and C2,6-H of the 4-methoxyphenyl moiety, respectively. The six protons of 4-methoxynaphthalen-1-yl moiety appeared as multiplet or doublet peak ($J=8.0$ Hz) in the region of δ 6.72–6.74 ppm and δ 7.42–8.29 ppm. Besides, the ^{13}C NMR spectrum of compound **5a** shown three peaks at δ 157.38–167.76 ppm, which attributed to the aromatic carbon connected with the amino or methoxy group. The signals observed at δ 103.78–146.16 ppm were assigned to aromatic carbons in the



- 3a** R₁ = 4-OCH₃ **3b** R₁ = 4-OC₂H₅ **3c** R₁ = 3,4,5-triOCH₃ **4a** R₁ = 4-OCH₃ **4b** R₁ = 4-OC₂H₅
4c R₁ = 2-Br-3,4,5-triOCH₃ **5a** R₁ = 4-OCH₃ **5b** R₁ = 4-OC₂H₅ **5c** R₁ = 2-Br-3,4,5-triOCH₃
6a R₁ = 4-OCH₃; R₂ = CH₃CO; R₃ = H **6h** R₁ = 4-OC₂H₅; R₂ = CH₃(C₂H₅)₂CO; R₃ = H
6b R₁ = 4-OCH₃; R₂ = C₂H₅CO; R₃ = H **6i** R₁ = 4-OC₂H₅; R₂ = (CH₃)₂CHCO; R₃ = H
6c R₁ = 4-OCH₃; R₂ = CH₃(C₂H₅)₂CO; R₃ = H **6j** R₁ = 2-Br-3,4,5-triOCH₃; R₂ = C₂H₅CO; R₃ = H
6d R₁ = 4-OCH₃; R₂ = Cl₃CCO; R₃ = H **6k** R₁ = 2-Br-3,4,5-triOCH₃; R₂ = (CH₃)₂CHCO; R₃ = H
6e R₁ = 4-OCH₃; R₂ = (CH₃)₂CHCO; R₃ = H **6l** R₁ = 2-Br-3,4,5-triOCH₃; R₂ = Cl₃CCO; R₃ = H
6f R₁ = 4-OC₂H₅; R₂ = CH₃CO; R₃ = H **6m** R₁ = 2-Br-3,4,5-triOCH₃; R₂ = R₃ = CH₃(C₂H₅)₂CO
6g R₁ = 4-OC₂H₅; R₂ = C₂H₅CO; R₃ = H **6n** R₁ = 2-Br-3,4,5-triOCH₃; R₂ = CH₃CO; R₃ = C₂H₅CO

Scheme 1. Reagents and conditions: (a) TFAA, TFA, room temperature, 12 h; (b) Pyridinium tribromide, CH₂Cl₂, r.t. 1 h; (c) Thiourea, EtOH, reflux, 3 h; (d) Acid anhydride, 120 °C, 3 h.

Table 1. Antiproliferative activities of target compounds (5a–5c and 6a–6n) on the human cancer cell lines.

Compound	R	IC ₅₀ (μM) ^a	
		MCF-7	A549
5a	R ₁ = 4-OCH ₃	1.80 ± 0.07	2.72 ± 0.18
5b	R ₁ = 4-OC ₂ H ₅	0.48 ± 0.03	0.97 ± 0.13
5c	R ₁ = 2-Br-3,4,5-triOCH ₃	31.05 ± 0.70	>50.0
6a	R ₁ = 4-OCH ₃ ; R ₂ = CH ₃ CO; R ₃ = H	2.16 ± 0.27	16.14 ± 0.83
6b	R ₁ = 4-OCH ₃ ; R ₂ = C ₂ H ₅ CO; R ₃ = H	14.75 ± 0.45	40.32 ± 0.32
6c	R ₁ = 4-OCH ₃ ; R ₂ = CH ₃ (C ₂ H ₅) ₂ CO; R ₃ = H	14.90 ± 0.34	>50.0
6d	R ₁ = 4-OCH ₃ ; R ₂ = Cl ₃ CCO; R ₃ = H	1.03 ± 0.09	1.91 ± 0.08
6e	R ₁ = 4-OCH ₃ ; R ₂ = (CH ₃) ₂ CHCO; R ₃ = H	12.27 ± 0.54	>50.0
6f	R ₁ = 4-OC ₂ H ₅ ; R ₂ = CH ₃ CO; R ₃ = H	5.49 ± 0.84	7.00 ± 0.30
6g	R ₁ = 4-OC ₂ H ₅ ; R ₂ = C ₂ H ₅ CO; R ₃ = H	9.61 ± 0.54	18.67 ± 0.89
6h	R ₁ = 4-OC ₂ H ₅ ; R ₂ = CH ₃ (C ₂ H ₅) ₂ CO; R ₃ = H	7.18 ± 0.78	>50.0
6i	R ₁ = 4-OC ₂ H ₅ ; R ₂ = (CH ₃) ₂ CHCO; R ₃ = H	7.69 ± 0.34	>50.0
6j	R ₁ = 2-Br-3,4,5-triOCH ₃ ; R ₂ = C ₂ H ₅ CO; R ₃ = H	>50.0	>50.0
6k	R ₁ = 2-Br-3,4,5-triOCH ₃ ; R ₂ = (CH ₃) ₂ CHCO; R ₃ = H	>50.0	>50.0
6l	R ₁ = 2-Br-3,4,5-triOCH ₃ ; R ₂ = Cl ₃ CCO; R ₃ = H	0.61 ± 0.06	0.92 ± 0.02
6m	R ₁ = 2-Br-3,4,5-triOCH ₃ ; R ₂ = R ₃ = CH ₃ (C ₂ H ₅) ₂ CO	>50.0	>50.0
6n	R ₁ = 2-Br-3,4,5-triOCH ₃ ; R ₂ = CH ₃ CO; R ₃ = C ₂ H ₅ CO	13.49 ± 0.82	16.31 ± 0.89
Cisplatin	–	11.15 ± 0.75	4.92 ± 0.56
5-Fu	–	11.61 ± 0.60	2.75 ± 0.31
Tamoxifen	–	14.28 ± 0.40	20.20 ± 0.65
CA-4	–	5.55 ± 0.11	0.029 ± 0.004

^aThe values given are means of three experiments.

compound. The peaks of two methoxy groups were observed at δ 55.30 ppm and δ 55.84 ppm, respectively. Furthermore, HRMS of compound **5a** showed a molecular ion peak at m/z 363.1126 as $[M + H]^+$ which also supports the proposed structure of the compound.

3. Biological evaluation

3.1. Antiproliferative activity

All newly prepared compounds were tested for their antiproliferative activity on the human breast cancer cell line (MCF-7) and

human lung adenocarcinoma cell line (A549) using the CCK-8 assay with cisplatin, 5-fluorouracil, tamoxifen, and CA-4 as the reference drugs. The results are expressed as IC_{50} values (50% inhibitory concentrations) and are summarised in Table 1. Except for compounds **5c**, **6j**, **6k**, and **6m**, the majority of the tested compounds exhibited moderate to potent antiproliferative activity. Among these compounds, compounds **5a**, **5b**, **6a**, **6d**, and **6l** displayed potent antiproliferative activity as compared to the standard drugs (cisplatin, 5-fluorouracil, tamoxifen, and CA-4). All other tested compounds (**6b**, **6c**, **6e–6j**, and **6n**) shown moderate inhibitory activity.

Based on the antiproliferative activities of these compounds, the structure-activity relationship (SAR) of this class of compounds is summarised. Compared the antiproliferative activity of **5a**, **5b**, and **5c**, the result was shown that the change of substituent affects the inhibitory activity. When the ethoxy group located at the para position of phenyl ring, the compound has the strongest activity (**5b**). The replacement of ethoxy group (**5b**) with methoxy group (**5a**) decreased the activity slightly. However, the replacement of 4-ethoxyphenyl (**5b**) with 2-bromo-3,4,5-trimethoxyphenyl (**5c**) resulted in a remarkable decrease of antiproliferative activity. Among this series of thiazole-naphthalene derivatives, compound **5b** with an ethoxy group at the 4-position of the phenyl ring and

free amine group at the thiazole ring, was found to be the most active compound. On the other hand, introduction of fatty acyl group into the aminothiazole resulting in significantly decreased antiproliferative activity, such as CH_3CO , C_2H_5CO , $CH_3(C_2H_5)_2CO$, and $(CH_3)_2CHCO$. It is interesting to point out that **6d** and **6l** containing the trichloroacetyl group (Cl_3CCO) at the aminothiazole moiety significantly improved the antiproliferative activity. In summary, the information of SAR provided us a guideline to improve the antiproliferative activity in future structural modification.

In order to evaluate the safety of this series of compounds, the most potent compound **5b** was selected to tested its inhibitory activity against normal human embryonic kidney cell line (HEK293). The results showed that compound **5b** showed low toxicity in human normal cell line ($IC_{50} = 16.37 \pm 4.61 \mu M$) compared to MCF-7 ($IC_{50} = 0.48 \pm 0.03 \mu M$) and A549 ($IC_{50} = 0.97 \pm 0.13 \mu M$) cancer cell lines. Hence, these compounds have good safety for potential application in the treatment of cancer.

3.2. In vitro tubulin polymerisation assay

To evaluate whether this series of compounds displayed anti-cancer activity by targeting tubulin-microtubule system, the *in vitro* tubulin polymerisation inhibitory activities of compounds **5b**, **6d**, and **6l** were evaluated using the method previously described²⁴. Meanwhile, colchicine (tubulin destabilising agent) was chosen as the positive control. As shown in Table 2, the tubulin inhibitory polymerisation (IC_{50}) of compounds **5b**, **6d**, and **6l** were 3.3 μM , 6.6 μM , and 4.0 μM , respectively. Considering the results of antiproliferative and *in vitro* tubulin inhibition activities, compound **5b** was selected to further discuss the mechanism of

Table 2. Tubulin inhibitory activities of compounds **5b**, **6d**, and **6l**.

Compound	Structure	IC_{50} (μM)
5b	$R_1 = 4-OCH_2CH_3$	3.3
6d	$R_1 = 4-OCH_3$; $R_2 = Cl_3CCO$; $R_3 = H$	6.6
6l	$R_1 = 2-Br-3,4,5-triOCH_3$; $R_2 = Cl_3CCO$; $R_3 = H$	4.0
Colchicine		9.1

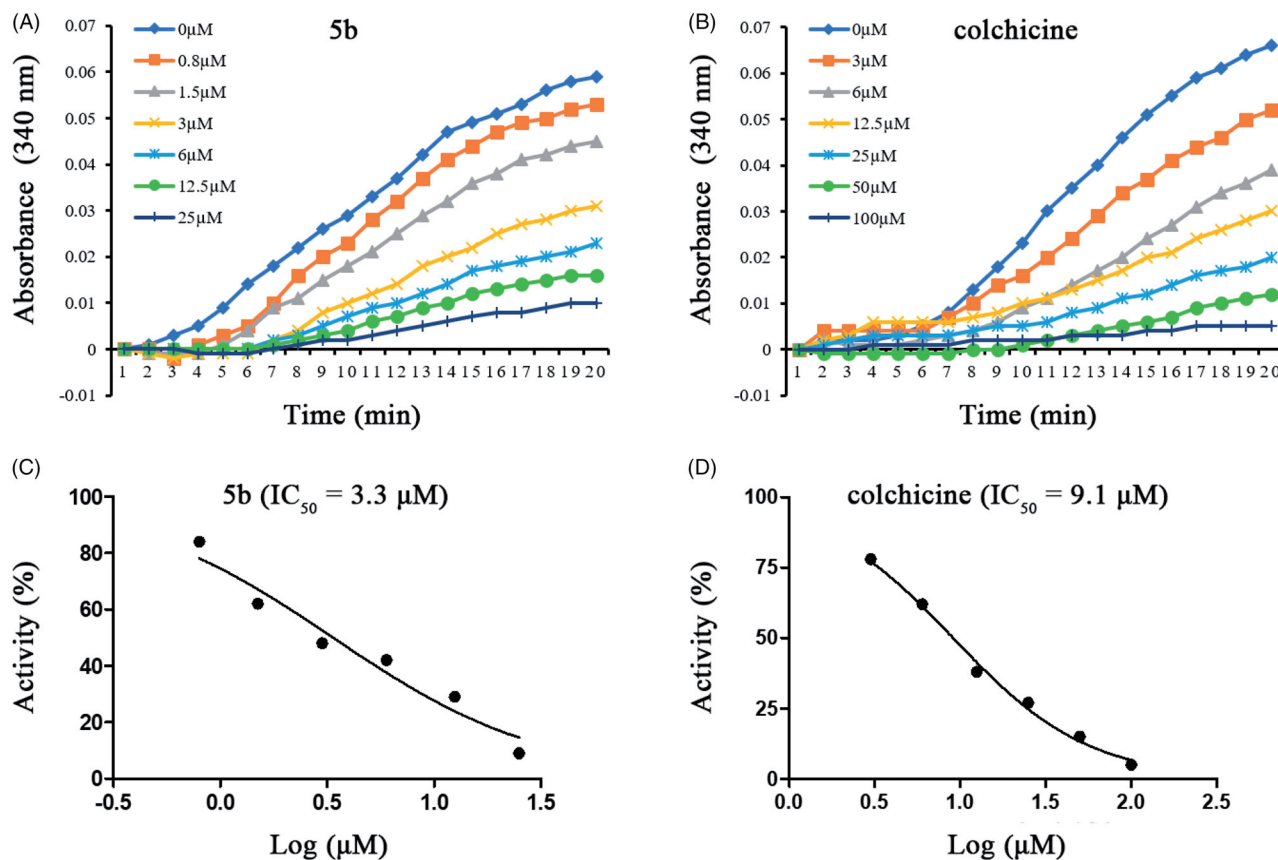


Figure 3. Tubulin polymerisation inhibitory activities of **5b** and colchicine. Purified tubulin protein was incubated at 37 °C in the absence or presence of **5b** (A,C) and colchicine (B,D) at the indicated concentrations.

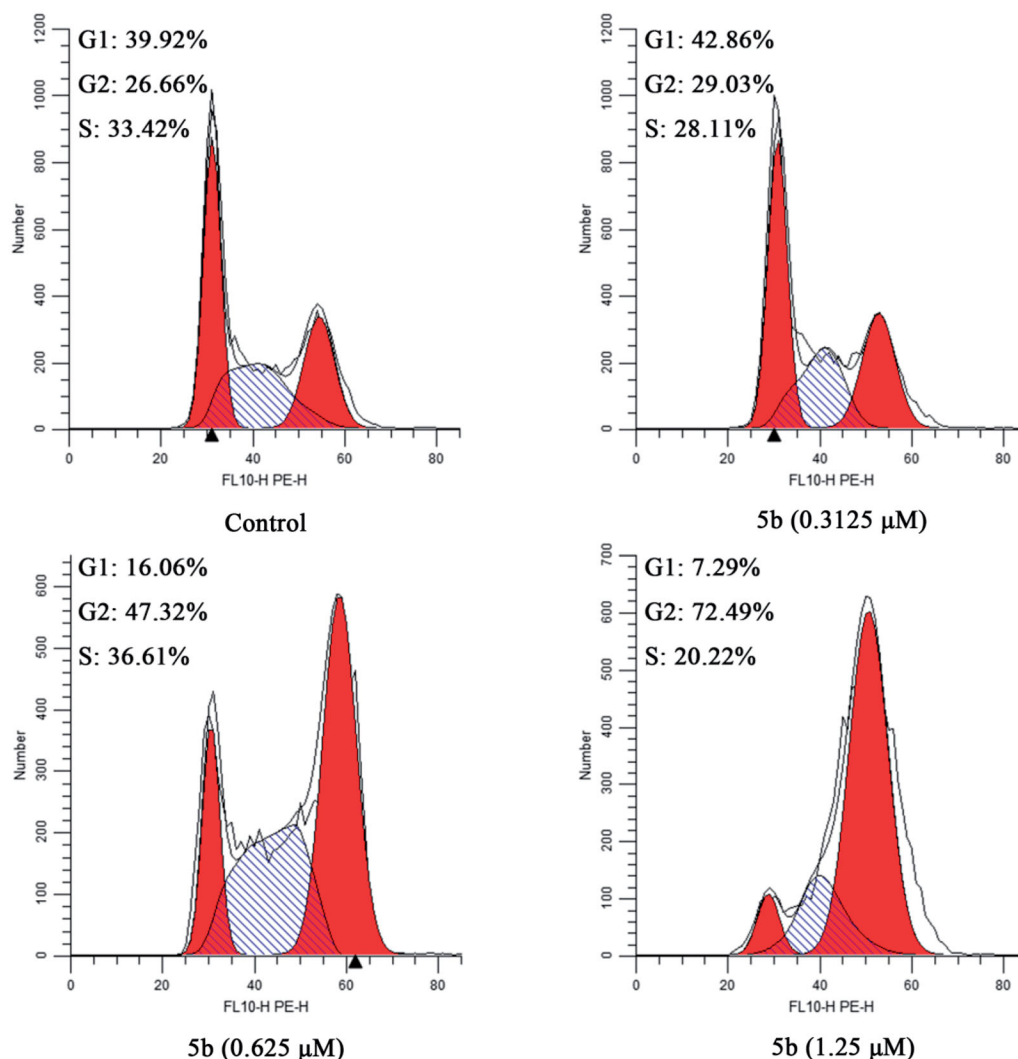


Figure 4. The cell cycle of MCF-7 cancer cells treated with different concentration of **5b** (0, 0.3125, 0.625, and 1.25 μM).

tubulin inhibition. As shown in Figure 3, compound **5b** exhibited similar action to that of colchicine. With the increase of the concentration of compound **5b** or colchicine, the fluorescence intensity of tubulin was obviously slowed down as compared with the control. These results indicated that **5b** was the tubulin destabilising agent with an IC_{50} value of 3.3 μM , which was superior to that of colchicine ($\text{IC}_{50} = 9.1 \mu\text{M}$). These data confirmed that the anti-proliferative activity of these compounds is related to their inhibition of tubulin polymerisation, and tubulin was the most likely the target of these compounds.

3.3. Cell cycle analysis

Based on the literature report, most tubulin destabilising agents can disrupt regulated cell cycle distribution and lead to cell cycle arrest at metaphase^{23,31}. Therefore, we evaluated the effect of the most promising compound **5b** on the cell cycle of MCF-7 cancer cells using the flow cytometry analysis assay. In this study, MCF-7 cancer cells were incubated with different concentrations of **5b** (0.3125, 0.625, and 1.25 μM) for 24 h. The results were shown in Figure 4, after the addition of different concentrations of **5b** (0.3125, 0.625, and 1.25 μM), the G2/M population increased from 26.66% (control) to 72.49% (1.25 μM). These findings demonstrated

that **5b** can arrest cell cycle at G2/M phase in a dose-dependent manner.

3.4. Induction of cellular apoptosis

Considering that tubulin polymerisation inhibitors can induce cellular apoptosis³², the Annexin V-FITC/PI assay was performed to detect whether compound **5b** was able to induce cancer cell apoptosis. After treatment with different concentrations of **5b** (0, 0.3125, 0.625, and 1.25 μM), the obtained data showed **5b** can initiate cellular apoptosis and dissipate cellular integrity. As shown in Figure 5, when MCF-7 cancer cells were incubated with **5b** at 0.3125, 0.625, or 1.25 μM for 24 h, the total numbers of early and late apoptotic cells were 15.78%, 25.6%, and 27.7%, respectively, whereas that of the control group was only 4.93%. These results implied that compound **5b** effectively induced cell apoptosis in MCF-7 cells via a dose-dependent manner.

3.5. Molecular docking

Molecular docking studies were carried out to elucidate the binding mode of this series of compounds with the colchicine binding site of tubulin. To verify the accuracy of the docking results, colchicine was first docked into the colchicine binding site of tubulin.

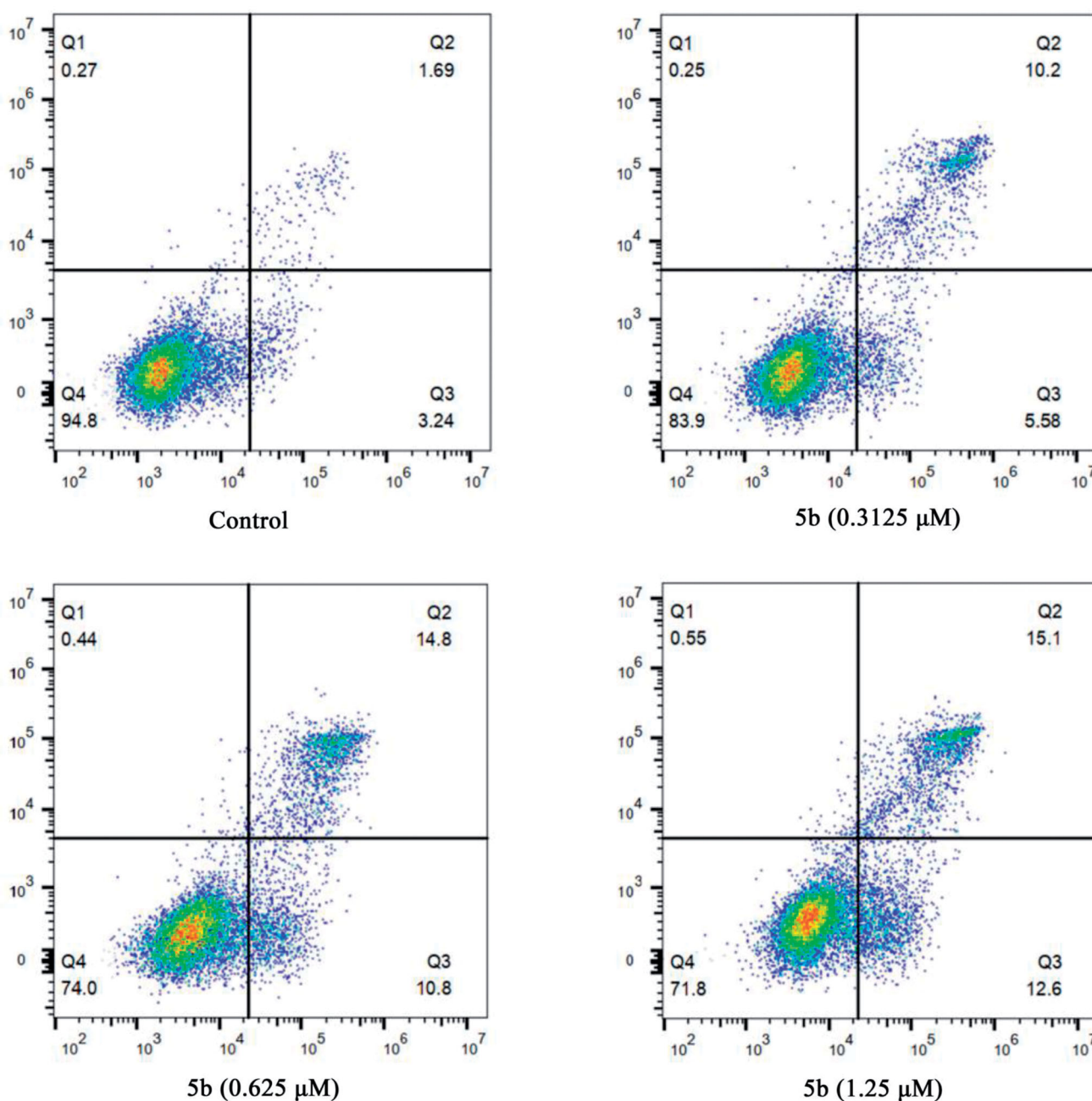


Figure 5. Flow cytometric analysis of apoptotic cells after treatment of MCF-7 cells with different concentrations of **5b** (0, 0.3125, 0.625, and 1.25 μ M).

The co-crystallized conformation of colchicine was reproduced approximately (RMSD: 1.083 Å), indicating that the protocol of molecular docking can reproduce the crystallographic pose of colchicine. Then, we investigate the theoretical binding mode of compound **5b** with tubulin. As shown in Figure 6, **5b** adopted an "L-shaped" conformation in the pocket of the tubulin with estimated binding energy of $-9.1 \text{ kcal}\cdot\text{mol}^{-1}$. The 4-methoxynaphthalene moiety of **5b** located at the hydrophobic pocket, surrounded by the residues A/Ala-180, A/Val-181, B/Leu-248, B/Ala-250, B/Leu-255, B/Met-259, B/Ala-316, B/Ala-317, B/Val-318 and B/Ala-354, forming a strong hydrophobic binding. Detailed analysis showed that the phenyl group of **5b** formed a cation- π interaction with the residue B/Lys-352. It was shown that the residue B/Asn-258 (bond length: 2.3 Å) formed a hydrogen bond with **5b**, which was the main interaction between **5b** and tubulin. All these interactions helped **5b** to anchor in the binding site of the tubulin.

3.6. Molecular dynamics (MD) simulations

To explore the potential binding mode between **5b** and the α,β -tubulin, molecular docking and molecular dynamics simulations were performed using the AutoDock vina 1.1.2 and Amber 12 software package. The preferential binding mechanism of α,β -tubulin with **5b** was determined by 30-ns molecular dynamics simulations based on the docking results. To explore the dynamic stability of the models and to ensure the rationality of the sampling strategy, the root-mean-square deviation (RMSD) value of the protein backbone based on the starting structure along the simulation time was calculated and plotted in Figure 7(A). As shown in Figure 7(A), the protein structure of the system was stabilised during the simulation.

The theoretical binding mode between **5b** and α,β -tubulin was shown in Figure 7(B). Compound **5b** adopted a compact

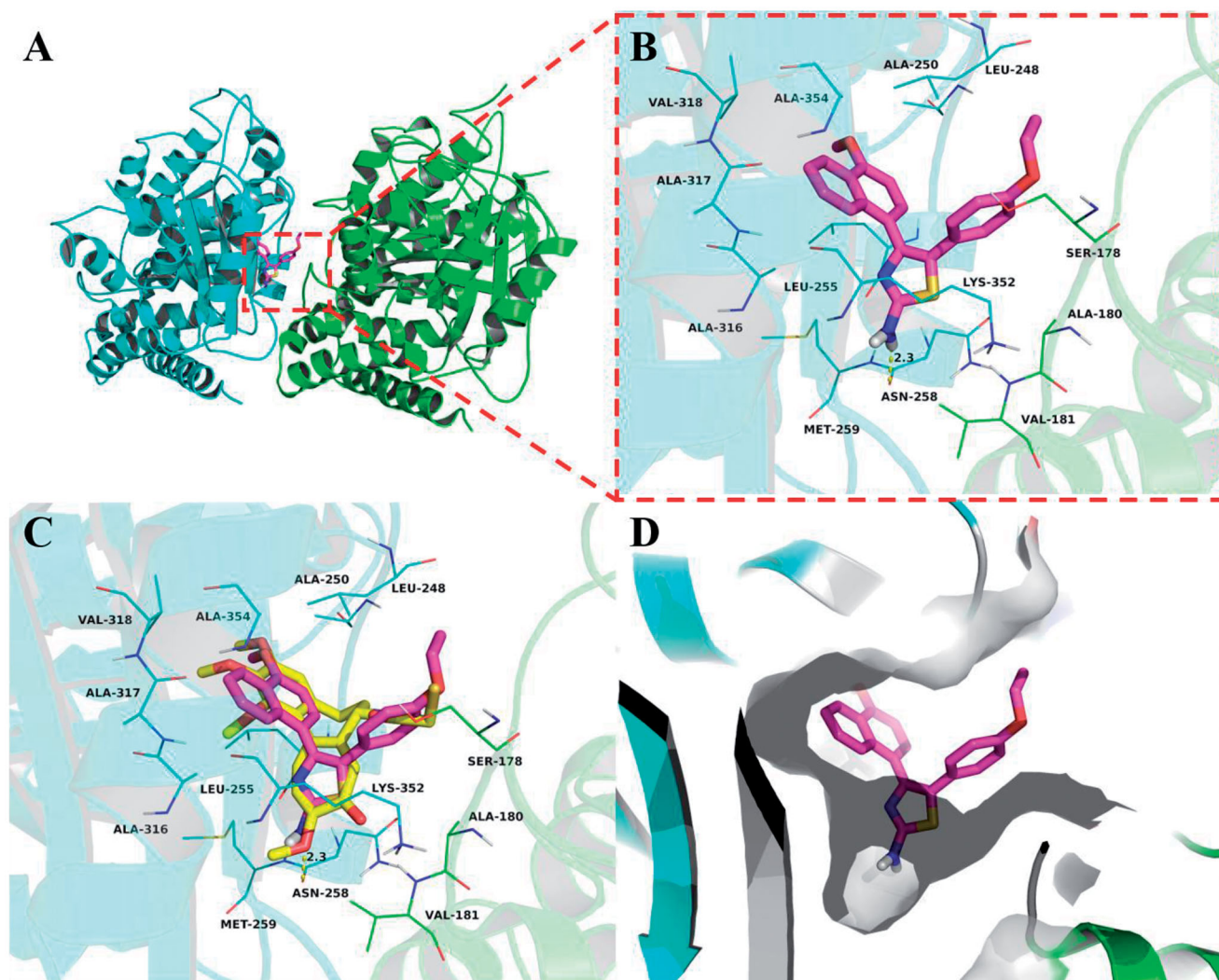


Figure 6. Compound **5b** was docked to the binding pocket of the α,β -tubulin (α : green; β : cyan). (A) Overall structure of α,β -tubulin with **5b**. (B) Binding pose of **5b** at colchicine binding site. (C) Superimposed pose of **5b** (pink) and colchicine (yellow) in the binding site. (D) Binding pose of **5b** in the surface of colchicine binding pocket.

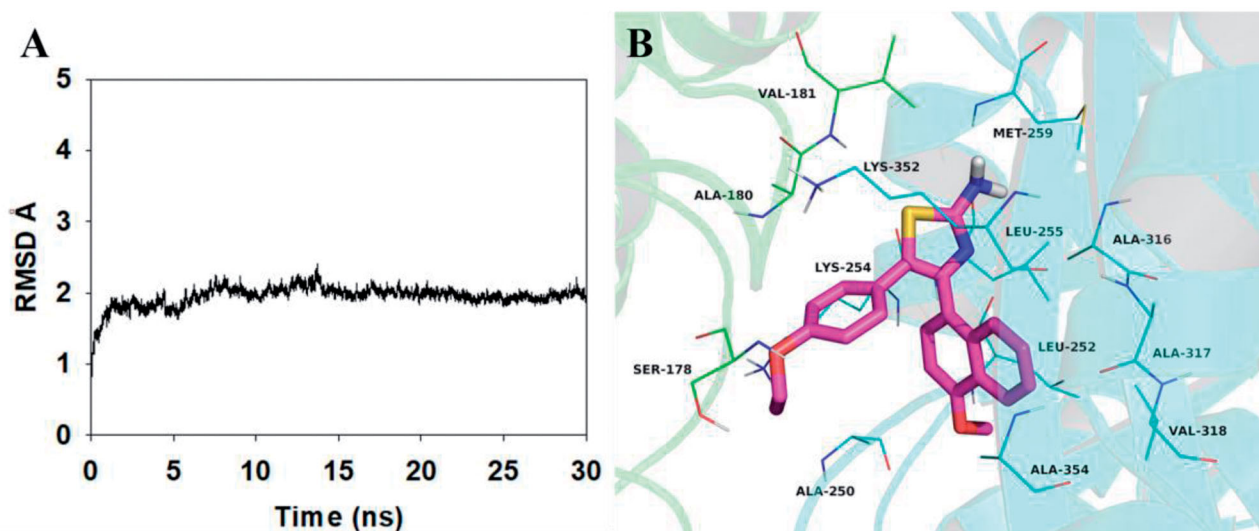


Figure 7. Molecular docking and molecular dynamics refinement of compound **5b** with tubulin. (A) The root-mean-square deviation (RMSD) of all the atoms of tubulin-**5b** complex with respect to its initial structure as function of time. (B) Molecular dynamics results of tubulin-**5b** complex.

conformation in the pocket of the α,β -tubulin. The compound **5b** located at the hydrophobic pocket, surrounded by the residues A/Ala-180, A/Val-181, B/Ala-250, B/Leu-252, B/Leu-255, B/Met-259, B/Ala-316, B/Ala-317, B/Val-318 and B/Ala-354, forming a strong hydrophobic binding. Detailed analysis showed that the phenyl group of **5b** formed cation- π interactions with the residues Lys-254 and Lys-352. All these interactions helped **5b** to anchor in the binding site of the α,β -tubulin. All in all, the above molecular dynamics simulation give us rational explanation of the interaction between **5b** and the α,β -tubulin, which provided valuable information for further development of α,β -tubulin inhibitors.

4. Conclusion

In summary, a novel series of thiazole-naphthalene derivatives (**5a–5c** and **6a–6n**) have been designed, synthesised, and characterised by various analytical techniques such as HRMS, ^1H NMR, and ^{13}C NMR. Antiproliferative activity of these newly prepared compounds was evaluated on the human breast cancer cell line (MCF-7) and human lung adenocarcinoma cell line (A549) using the CCK-8 assay. Amongst all the tested compounds, compound **5b** containing an ethoxy group at the 4-position of the phenyl ring and free amine group at the thiazole ring was found to be the most active compound with IC_{50} values of 0.48 ± 0.03 and $0.97 \pm 0.13 \mu\text{M}$. Mechanistic studies revealed that **5b** significantly inhibited tubulin polymerisation with an IC_{50} value of $3.3 \mu\text{M}$. Cellular mechanism studies elucidated that **5b** arrested the cell cycle at G2/M phase and induced apoptosis in MCF-7 cancer cells. Furthermore, molecular docking study indicated that **5b** binds well to the colchicine binding site of tubulin.

Disclosure statement

No potential conflict of interest was reported by the author(s).

Funding

This work was supported by the One Thousand Talents Program of Guizhou Province (the fifth group, [2019]4), Science and Technology Fund of Guizhou Health Commission (gzwjkj2019-1-183), Academic New Seedling Project of Guizhou Medical University (19NSP030).

ORCID

Guangcheng Wang  <http://orcid.org/0000-0001-9104-337X>

References

- Jordan MA, Wilson L. Microtubules as a target for anticancer drugs. *Nat Rev Cancer* 2004;4:253–65.
- Sorger PK, Dobles M, Tournebize R, et al. Coupling cell division and cell death to microtubule dynamics. *Curr Opin Cell Biol* 1997;9:807–14.
- Downing KH, Nogales E. Tubulin structure: insights into microtubule properties and functions. *Curr Opin Struct Biol* 1998;8:785–91.
- Schwartz EL. Antivascular actions of microtubule-binding drugs. *Clin Cancer Res* 2009;15:2594–601.
- Amos LA. Microtubule structure and its stabilisation. *Org Biomol Chem* 2004;2:2153–60.
- Pasquier E, André N, Braguer D. Targeting microtubules to inhibit angiogenesis and disrupt tumour vasculature: Implications for cancer treatment. *Curr Cancer Drug Targets* 2007;7:566–81.
- Shao Y-Y, Yin Y, Lian B-P, et al. Synthesis and biological evaluation of novel shikonin-benzo[b]furan derivatives as tubulin polymerization inhibitors targeting the colchicine binding site. *Eur J Med Chem* 2020;190:112105.
- Sigalapalli DK, Pooladanda V, Singh P, et al. Discovery of certain benzyl/phenethyl thiazolidinone-indole hybrids as potential anti-proliferative agents: Synthesis, molecular modeling and tubulin polymerization inhibition study. *Bioorg Chem* 2019;92:103188.
- Stanton RA, Gernert KM, Nettles JH, et al. Drugs that target dynamic microtubules: a new molecular perspective. *Med Res Rev* 2011;31:443–81.
- Dumontet C, Jordan MA. Microtubule-binding agents: a dynamic field of cancer therapeutics. *Nat Rev Drug Discov* 2010;9:790–803.
- Kaur R, Kaur G, Gill RK, et al. Recent developments in tubulin polymerization inhibitors: an overview. *Eur J Med Chem* 2014;87:89–124.
- Gümüş M, Yakan M, Koca İ. Recent advances of thiazole hybrids in biological applications. *Future Med Chem* 2019; 11:1979–98.
- Mishra R, Sharma PK, Verma PK, et al. Biological potential of thiazole derivatives of synthetic origin. *J Heterocycl Chem* 2017;54:2103–16.
- Chhabria MT, Patel S, Modi P, et al. Thiazole: a review on chemistry, synthesis and therapeutic importance of its derivatives. *Curr Top Med Chem* 2016;16:2841–62.
- Sharma PC, Bansal KK, Sharma A, et al. Thiazole-containing compounds as therapeutic targets for cancer therapy. *Eur J Med Chem* 2020;188:112016.
- Ayati A, Emami S, Moghimi S, et al. Thiazole in the targeted anticancer drug discovery. *Future Med Chem* 2019;11: 1929–52.
- Jain S, Pattnaik S, Pathak K, et al. Anticancer potential of thiazole derivatives: a retrospective review. *Mini Rev Med Chem* 2018;18:640–55.
- Ohsumi K, Hatanaka T, Fujita K, et al. Syntheses and antitumor activity of cis-restricted combretastatins: 5-membered heterocyclic analogues. *Bioorg Med Chem Lett* 1998;8: 3153–8.
- Sun ML, Xu QL, Xu JW, et al. Synthesis and bioevaluation of *N*,4-diaryl-1,3-thiazole-2-amines as tubulin inhibitors with potent antiproliferative activity. *PLoS One* 2017;12:e0174006.
- Shaik TB, Hussaini SMA, Nayak VL, et al. Rational design and synthesis of 2-anilinopyridinyl-benzothiazole schiff bases as antimetabolic agents. *Bioorg Med Chem Lett* 2017;27:2549–58.
- Salehi M, Amini M, Ostad SN, et al. Synthesis, cytotoxic evaluation and molecular docking study of 2-alkylthio-4-(2,3,4-trimethoxyphenyl)-5-aryl-thiazoles as tubulin polymerization inhibitors. *Bioorg Med Chem* 2013;21:7648–54.
- Wang G, Peng Z, Zhang J, et al. Synthesis, biological evaluation and molecular docking studies of aminochalcone derivatives as potential anticancer agents by targeting tubulin colchicine binding site. *Bioorg Chem* 2018;78:332–40.
- Wang G, Liu W, Gong Z, et al. Synthesis, biological evaluation, and molecular modelling of new naphthalene-chalcone derivatives as potential anticancer agents on MCF-7 breast cancer cells by targeting tubulin colchicine binding site. *J Enzyme Inhib Med Chem* 2020;35:139–44.

24. Wang G, Liu W, Tang J, et al. Design, synthesis, and anti-cancer evaluation of benzophenone derivatives bearing naphthalene moiety as novel tubulin polymerization inhibitors. *Bioorg Chem* 2020;104:104265.
25. Maya ABS, Perez-Melero C, Mateo C, et al. Further naphthyl-combretastatins. An investigation on the role of the naphthalene moiety. *J Med Chem* 2005;48:556–68.
26. Wang G, Qiu J, Xiao X, et al. Synthesis, biological evaluation and molecular docking studies of a new series of chalcones containing naphthalene moiety as anticancer agents. *Bioorg Chem* 2018;76:249–57.
27. Viegas-Junior C, Danuello A, VdS B, et al. Molecular hybridization: a useful tool in the design of new drug prototypes. *Curr Med Chem* 2007;14:1829–52.
28. Ivasiv V, Albertini C, Goncalves AE, et al. Molecular hybridization as a tool for designing multitarget drug candidates for complex diseases. *Curr Top Med Chem* 2019;19:1694–711.
29. Wang XD, Wei W, Wang PF, et al. Novel 3-arylfuran-2(5h)-one-fluoroquinolone hybrid: design, synthesis and evaluation as antibacterial agent. *Bioorg Med Chem* 2014;22:3620–8.
30. Xiao ZP, Wang XD, Wang PF, et al. Design, synthesis, and evaluation of novel fluoroquinolone-flavonoid hybrids as potent antibiotics against drug-resistant microorganisms. *Eur J Med Chem* 2014;80:92–100.
31. Hao S-Y, Qi Z-Y, Wang S, et al. Synthesis and bioevaluation of *n*-(3,4,5-trimethoxyphenyl)-1*h*-pyrazolo[3,4-*b*]pyridin-3-amines as tubulin polymerization inhibitors with anti-angiogenic effects. *Bioorg Med Chem* 2021;31:115985.
32. Mustafa M, Anwar S, Elgamal F, et al. Potent combretastatin a-4 analogs containing 1,2,4-triazole: Synthesis, antiproliferative, anti-tubulin activity, and docking study. *Eur J Med Chem* 2019;183:111697.